PCP
PLANT & CELL PHYSIOLOGY

Comparative Analysis of MAMP-induced Calcium Influx in *Arabidopsis* Seedlings and Protoplasts

Jens Maintz[1], Meltem Cavdar[2], Janina Tamborski[2], Mark Kwaaitaal[1], Rik Huisman[1,4], Christian Meesters[3], Erich Kombrink[3] and Ralph Panstruga[1,2,*]

[1]Max Planck Institute for Plant Breeding Research, Department of Plant–Microbe Interactions, Carl-von-Linné-Weg 10, 50829 Cologne, Germany
[2]RWTH Aachen University, Institute for Biology I, Unit of Plant Molecular Cell Biology, 52056 Aachen, Germany
[3]Max Planck Institute for Plant Breeding Research, Chemical Biology Laboratory, Carl-von-Linné-Weg 10, 50829 Cologne, Germany
[4]Present address: Wageningen University, Laboratory of Molecular Biology, Droevendaalsesteeg 1, 6708 PB Wageningen, The Netherlands
*Corresponding author: E-mail, panstruga@bio1.rwth-aachen.de; Tel., +49-241-8026655; Fax, +49-241-8022637.
(Received January 27, 2014; Accepted August 14, 2014)

Rapid transient elevation of cytoplasmic calcium (Ca^{2+}) levels in plant cells is an early signaling event triggered by many environmental cues including abiotic and biotic stresses. Cellular Ca^{2+} levels and their alterations can be monitored by genetically encoded reporter systems such as the bioluminescent protein, aequorin. Employment of proteinaceous Ca^{2+} sensors is usually performed in transgenic lines that constitutively express the reporter construct. Such settings limit the usage of these Ca^{2+} biosensors to particular reporter variants and plant genetic backgrounds, which can be a severe constraint in genetic pathway analysis. Here we systematically explored the potential of *Arabidopsis thaliana* leaf mesophyll protoplasts, either derived from a transgenic apoaequorin-expressing line or transfected with apoaequorin reporter constructs, as a complementary biological resource to monitor cytoplasmic changes of Ca^{2+} levels in response to various biotic stress elicitors. We tested a range of endogenous and pathogen-derived elicitors in seedlings and protoplasts of the corresponding apoaequorin-expressing reporter line. We found that the protoplast system largely reflects the Ca^{2+} signatures seen in intact transgenic seedlings. Results of inhibitor experiments including the calculation of IC_{50} values indicated that the protoplast system is also suitable for pharmacological studies. Moreover, analyses of Ca^{2+}signatures in mutant backgrounds, genetic complementation of the mutant phenotypes and expression of sensor variants targeted to different subcellular localizations can be readily performed. Thus, in addition to the prevalent use of seedlings, the leaf mesophyll protoplast setup represents a versatile and convenient tool for the analysis of Ca^{2+} signaling pathways in plant cells.

Keywords: Aequorin • *Arabidopsis thaliana* • Calcium signature • Elicitor • flg22 • Lanthanum chloride • Staurosporine • Mesophyll protoplasts • Transfection.

Abbreviations: DAMP, danger-/damage-associated molecular pattern; LPS, lipopolysaccharide; MAMP, microbe-associated molecular pattern; MAPK, mitogen-activated protein kinase; PRR, pattern recognition receptor; RLK, receptor-like kinase.

Introduction

In eukaryotic cells, calcium (Ca^{2+}) ions act as important second messengers that regulate many cellular processes. In plant cells, cytoplasmic Ca^{2+} concentrations ($[Ca^{2+}]_{cyt}$) are generally kept low, but certain abiotic (light, cold, heat, drought) and biotic (infection, elicitor treatment) stimuli can induce a rapid transient increase in $[Ca^{2+}]_{cyt}$ by influx of Ca^{2+} from the extracellular environment or by release from internal stores (McAinsh and Pittman 2009). The recognition of microbe- or danger-/damage-associated molecular patterns (MAMPs or DAMPs, respectively) by specific pattern recognition receptors (PRRs), is known to trigger characteristic Ca^{2+} signatures (Lecourieux et al. 2006, Aslam et al. 2009). PRRs represent crucial components of plant innate immunity. Typically, they are receptor-like kinases (RLKs) anchored in the plasma membrane and comprise an N-terminal extracellular domain for ligand binding, a transmembrane domain, and a C-terminal cytoplasmic kinase domain for intracellular signaling. Several PRRs of the dicotyledonous model plant *Arabidopsis thaliana* have been characterized in detail, including FLAGELLIN SENSING 2 (FLS2) and ELONGATION FACTOR-THERMO UNSTABLE RECEPTOR (EFR), which activate downstream signaling upon detection of peptide epitopes of bacterial flagellin (flg22) and EF-Tu (elf18), respectively (Gómez-Gómez and Boller 2000, Zipfel et al. 2004). Similarly, chitin oligomers originating from fungal cell walls are recognized by direct binding to the PRR CHITIN ELICITOR RECEPTOR KINASE 1 (CERK1) (Miya et al. 2007, Liu et al. 2012, Petutschnig et al. 2010), whereas the receptor for lipopolysaccharides (LPS), originating from the outer membrane of Gram-negative bacteria, has not yet been identified (Newman et al. 2013). In *Arabidopsis* the DAMPs Pep1 through Pep6 serve as endogenous elicitors, which are short peptides stimulating innate immune responses (Huffaker et al. 2006). The PRR PEPTIDE RECEPTOR 1 (PEPR1) functions as receptor for Pep1-Pep6, whereas PEPR2 acts as a receptor for Pep1 and Pep2 (Yamaguchi et al. 2010). The RLK BRASSINOSTEROID INSENSITIVE 1–ASSOCIATED RECEPTOR KINASE 1 (BAK1) does not directly bind MAMPs/DAMPs, but serves as a co-receptor for FLS2, EFR, PEPR1/PEPR2 and possibly other

Regular Paper

Plant Cell Physiol. 55(10): 1813–1825 (2014) doi:10.1093/pcp/pcu112, Advance Access publication on 16 September 2014, available online at www.pcp.oxfordjournals.org

PRRs (Kim et al. 2013). A set of canonical cellular responses is typically initiated by activation of PRRs, including extracellular alkalization (Felix et al. 1999), rapid transient increase of $[Ca^{2+}]_{cyt}$ (Aslam et al. 2009, Jeworutzki et al. 2010), activation of Ca^{2+}-dependent protein kinases (CDPKs; Boudsocq et al. 2010), generation of reactive oxygen species (ROS, Felix et al. 1999), alterations in lateral plasma membrane organization (Keinath et al. 2010), initiation of mitogen-activated protein kinase (MAPK(K/KK)) cascades (Asai et al. 2002), and transcriptional activation of a set of defense-related genes (Zipfel et al. 2004). Although a range of candidate Ca^{2+} channels in plants is known (Wheeler and Brownlee 2008), the molecular identity of the channels mediating the MAMP/DAMP-induced cellular Ca^{2+} influx in plants remains elusive. Previous pharmacological studies suggest a significant contribution of ionotropic glutamate receptor (iGluR)-like channels to this process (Kwaaitaal et al. 2011, Vatsa et al. 2011a, Kwaaitaal et al. 2012); however, genetic evidence in support of this possibility has only recently emerged (Li et al. 2013, Manzoor et al. 2013).

There exist a number of methods to measure steady-state levels and dynamics of $[Ca^{2+}]_{cyt}$ in plants. One commonly used procedure employs the genetically encoded proteinaceous bioluminescent Ca^{2+} sensor apoaequorin from the jellyfish *Aequorea victoria*. The complex formed between apoaequorin and its prosthetic group, the luciferin coelenterazine, is termed aequorin, which upon binding of three Ca^{2+} ions emits light at a wavelength of 470 nm. The emitted light can be quantified as bioluminescence *via* photomultiplier tubes or charge-coupled devices (Knight et al. 1991). Using microplate readers for bioluminescence quantification, Ca^{2+} measurements on the basis of aequorin are suitable for medium- to high-throughput screening (Ranf et al. 2012). By decreasing sample size and increasing the rate of data collection in individual samples, it is possible to obtain high-resolution kinetics with good reproducibility. Such measurements can be useful to discover even small phenotypic changes in mutant lines or pharmacologically treated samples.

A marked disadvantage of the bioluminescent aequorin Ca^{2+} reporter system and other genetically encoded Ca^{2+} sensors is the need for integration of the respective biosensor constructs into suitable plant lines by either transformation or crossing, which are both laborious and time-consuming. An attractive alternative to stable integration of the reporter systems into plant genomes is transient expression of the respective constructs. Various transient expression systems have been established for plants, including particle bombardment (Panstruga 2004), *Agrobacterium tumefaciens*-mediated expression (Gelvin 2003) and protoplast transfection (Davey et al. 2005, Yoo et al. 2007). Especially the latter method has been widely used and seminal results have been obtained on the basis of *Arabidopsis* leaf mesophyll protoplasts. This includes, for example, the elucidation of MAMP-triggered MAPK cascades (Asai et al. 2002) and the functional analysis of defense signaling *via* Ca^{2+}-dependent protein kinases (Boudsocq et al. 2010).

Protoplast- and cell culture-based Ca^{2+} measurements using the apoaequorin reporter have been performed in *Arabidopsis* (Demidchik et al. 2004, Carpaneto et al. 2007, Jeworutzki et al. 2010), but also in other plant systems such as tobacco (Haley et al. 1995, Mazars et al. 1997, Lecourieux et al. 2005), parsley (Blume et al. 2000), rice (Kurusu et al. 2011), barley and carrot (Gilroy et al. 1989). Typically, Ca^{2+} quantification was combined with a variety of abiotic and biotic stress stimuli. However, the validity of this approach has so far not been proven by systematic direct comparison of the protoplast-derived responses with those obtained with the corresponding intact plant systems; in particular, there have been no previous reports on MAMP-/DAMP-induced Ca^{2+} signatures in *Arabidopsis* protoplasts.

Here we report on Ca^{2+} measurements on the basis of transient expression of the Ca^{2+} biosensor apoaequorin in *Arabidopsis thaliana* leaf mesophyll protoplasts. We systematically compared MAMP- and DAMP-induced Ca^{2+} signatures recorded in the protoplast system with those obtained in seedlings of stable transgenic plant lines, both in the context of pharmacological inhibitor and genetic complementation experiments. Our data demonstrate that MAMP-/DAMP-triggered Ca^{2+} transients in leaf mesophyll protoplasts are overall comparable to the responses seen in intact seedlings. We conclude that the leaf protoplast system is suitable for pharmacological and genetic analysis of MAMP-/DAMP-induced Ca^{2+} signatures. Our study thus provides a solid basis for the future application of protoplast-based measurements of Ca^{2+} signatures using the aequorin sensor in *Arabidopsis* as well as in other plant species.

Results

Arabidopsis leaf mesophyll protoplasts are responsive to various elicitors

To find out whether the Ca^{2+} signature in leaf mesophyll protoplasts reflects the Ca^{2+} response seen in intact plant seedlings, we first isolated protoplasts from rosette leaves of the transgenic *Arabidopsis* line, Col-0 [pMAQ2], which expresses the apoprotein of the Ca^{2+} sensor aequorin in the plant cytoplasm (Knight et al. 1991). To compensate for the lack of the apoplastic Ca^{2+} store present in intact plant tissues, we incubated protoplasts in buffer containing 2 mM Ca^{2+}, which is within the $[Ca^{2+}]$ range typically found in the plant extracellular space (10 μM to 10 mM; Bush 1995, Stael et al. 2012). Subsequently, the leaf mesophyll protoplasts were challenged with different MAMPs and DAMPs and changes in $[Ca^{2+}]_{cyt}$ were recorded over time. Results were compared to data obtained in parallel experiments employing intact seedlings of the transgenic Col-0 [pMAQ2] line grown in hydroponic culture.

The kinetic properties of the flg22-induced cytoplasmic Ca^{2+} transients observed in mesophyll protoplasts were comparable to the ones monitored with *Arabidopsis* seedlings, with minor differences. In both systems treatment with flg22 caused a rapid transient increase in $[Ca^{2+}]_{cyt}$. The Ca^{2+} spike, which was nearly identical in amplitude in both systems ($\Delta[Ca^{2+}]_{cyt}$ ca. 120–130 nM; **Figs. 1a** and **2a**; note that absolute values are

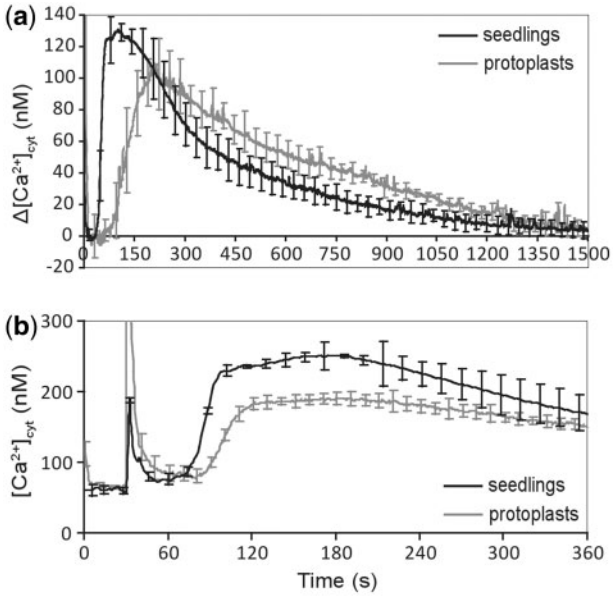

Fig. 1 flg22-induced Ca^{2+}signatures are similar in *Arabidopsis* seedlings and mesophyll leaf protoplasts. *Arabidopsis* seedlings of the apoaequorin-expressing Col-0 [pMAQ2] line grown in hydroponic culture (black curves) and leaf mesophyll protoplasts derived from this line (gray curves) were treated with 1 μM flg22 at the start of the measurements (a) or at 30 s after the beginning of the measurements (b). Luminescence was followed over time and absolute $[Ca^{2+}]_{cyt}$ calculated as previously described (Rentel and Knight 2004). Presented curves focus either on the peak and recovery phase in a 25-minute time course (a) or on the injection peak preceding the flg22-induced response in a 6-minute time interval (b). Data represent absolute $[Ca^{2+}]_{cyt}$ (b) or $\Delta[Ca^{2+}]_{cyt}$ (a) after normalization to steady state Ca^{2+} levels after MAMP addition and decay of the injection spike, i.e. prior to the genuine elicitor-triggered Ca^{2+} response. Curves are from representative experiments each showing the mean (±SD) of three technical replicates.

subject to experimental variation), was followed by a slow and gradual decrease during the recovery phase (**Fig. 1a**). While in intact seedlings the $[Ca^{2+}]_{cyt}$ started to increase at about 40 s after administration of flg22 and typically reached a maximum at 60 to 120 s, the response of protoplasts was slightly delayed. In protoplasts, Ca^{2+}influx started at ca. 60 s and maximum $[Ca^{2+}]_{cyt}$ was reached at about 120 to 180 s (**Figs. 1** and **2a**). The kinetics of the recovery phase was similar in seedlings and protoplasts; in both systems $[Ca^{2+}]_{cyt}$ declined back to resting levels at ca. 25 min (1500 s) after treatment with flg22 (**Fig. 1a**). In seedlings, $[Ca^{2+}]_{cyt}$ dropped rapidly and then slowly phased out, typically resulting in a concavely shaped recovery curve (Kwaaitaal et al. 2011, Ranf et al. 2011, Ranf et al. 2012), whereas in protoplasts the decrease in $[Ca^{2+}]_{cyt}$ was less steep and steadier (**Fig. 1a**).

A characteristic feature of the experimentally determined Ca^{2+} signature is the so-called 'injection peak', which is presumably caused by physical perturbation of the system upon injection of the MAMP solution into microplate wells harboring the apoaequorin-expressing specimen. Injection may also cause the generation of ion microgradients, osmotic effects or temperature changes, which collectively may be responsible for this frequently observed and variable response (Kwaaitaal et al. 2011, Ranf et al. 2011). In both protoplasts and seedlings, this peak occurred instantly after MAMP injection, indicating that both systems are equally responsive to such perturbations (**Fig. 1b**; note that the amplitude of the injection peak is variable and subject to experimental variation). Resting levels of $[Ca^{2+}]_{cyt}$ prior to MAMP application were similar ($[Ca^{2+}]_{cyt}$ ca. 70 nM) in seedlings and protoplasts (**Fig. 1b**) and comparable to previously reported values in *Arabidopsis* seedlings that were also quantified by apoaequorin-based measurements (Aslam et al. 2009, Jeworutzki et al. 2010, Ranf et al. 2011, Kwaaitaal et al. 2012), whereas somewhat higher $[Ca^{2+}]_{cyt}$ were determined in plant protoplasts using Ca^{2+} indicator dyes (Gilroy et al. 1986, Gilroy et al. 1989).

We next assessed a range of additional MAMPs and DAMPs as triggers of $[Ca^{2+}]_{cyt}$ signatures. These included, in addition to flg22, the bacterial peptide MAMP elf18, the plant peptide DAMP Pep1, the fungal cell wall carbohydrate MAMP, chitin, and the bacterial cell wall MAMP, LPS. Previous measurements have shown the responsiveness of seedlings grown in hydroponic culture to these elicitors (Gust et al. 2007, Kwaaitaal et al. 2011, Kwaaitaal et al. 2012, Ranf et al. 2011, Ranf et al. 2012). In protoplasts, each of these MAMPs/DAMPs caused a rapid and transient increase in $[Ca^{2+}]_{cyt}$ (**Fig. 2**). The elf18-induced cytoplasmic Ca^{2+} transient in protoplasts was of similar amplitude as in seedlings ($\Delta[Ca^{2+}]_{cyt}$ ca. 80 nM), yet was delayed and showed a slower increase of the Ca^{2+} influx (**Fig. 2b**). By contrast, the Ca^{2+} signatures induced by Pep1 (**Fig. 2c**) or chitin (**Fig. 2d**) occurred at the same rate in protoplasts and seedlings, but the amplitudes were significantly higher in protoplasts when compared to seedlings (130–190 nM *versus* 70–80 nM), and the decline during the recovery phase happened earlier and proceeded faster (**Fig. 2c** and **d**). Finally, bacterial LPS induced a rapid Ca^{2+} transient only in protoplasts, but not in seedlings, where LPS caused no noticeable increase in $[Ca^{2+}]_{cyt}$ during the time of examination (**Fig. 2e**), comparable to the injection of solvent (water).

In summary, we found that the *Arabidopsis* protoplast system is responsive to all tested MAMPs/DAMPs, including flg22, elf18, Pep1, chitin, and LPS, but show $[Ca^{2+}]_{cyt}$ kinetics with some distinctive features regarding timing, amplitude and recovery phases compared to intact seedlings.

Pharmacological inhibition of flg22-induced $[Ca^{2+}]_{cyt}$ transients in *Arabidopsis* mesophyll protoplasts

Pharmacological inhibition is a common and often straightforward experimental approach to interfere with biological processes. It may provide meaningful insights into the underlying signaling pathways and can be applied at small scale (individual substances) or in high-throughput screens (compound libraries), an experimental approach known as chemical genetics (McCourt and Desveaux 2010). To find out whether aequorin-based Ca^{2+} measurements in leaf mesophyll protoplast are suitable for and react in a similar fashion to

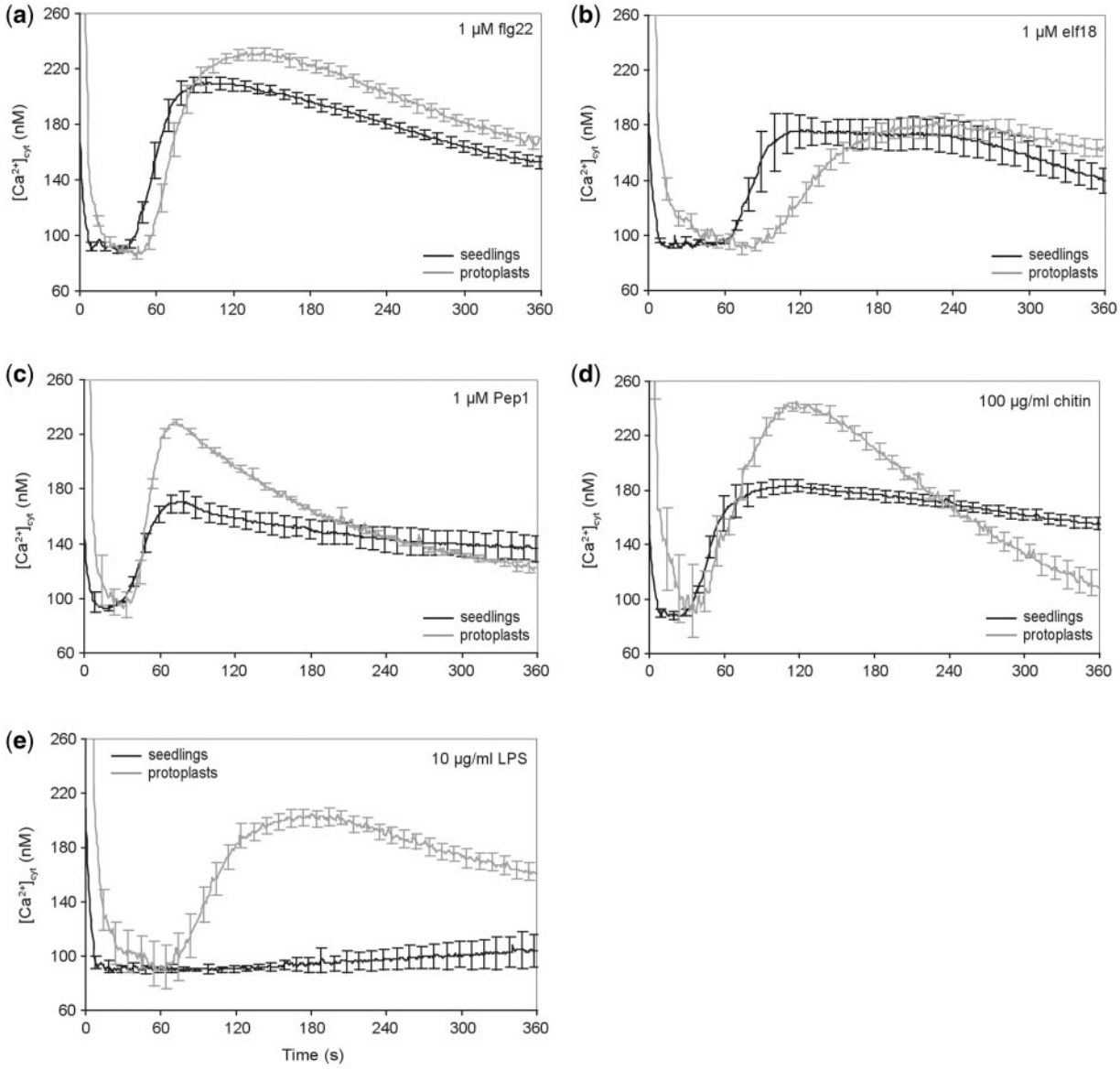

Fig. 2 The Ca^{2+} signature triggered by various MAMPs and DAMPs is similar in *Arabidopsis* seedlings and mesophyll leaf protoplasts. *Arabidopsis* seedlings of the apoaequorin-expressing Col-0 [pMAQ2] line grown in hydroponic culture (black curves) or leaf mesophyll protoplasts isolated from the transgenic apoaequorin-expressing Col-0 [pMAQ2 line] (gray curves) were treated with 1 μM flg22 (a), 1 μM elf18 (b), 1 μM Pep1 (c), 100 μg/ml chitin (d) or 10 μg/ml LPS (e) at the start of the measurements. Curves are from representative experiments each showing the mean (± SEM) of three biological replicates, all of which are based on at least three technical replicates, respectively. Since protoplast measurements of this set of experiments were performed in single wells to avoid physical perturbation by movement of the microplates, kinetic measurements were restricted to 6 minutes each.

pharmacological interference, we pretreated transgenic Col–0 [pMAQ2] seedlings and protoplasts with various concentrations of the non-selective Ca^{2+} channel blocker, lanthanum chloride ($LaCl_3$), or the pan-specific kinase inhibitor, staurosporine. Both $LaCl_3$ and staurosporine have previously been shown to effectively block cytoplasmic Ca^{2+} signatures in various experimental contexts and plant systems (Knight et al. 1997, Mazars et al. 1997, Lecourieux et al. 2002, Rentel and Knight 2004, Lecourieux et al. 2005, Vadassery et al. 2009, Kurusu et al. 2011, Kwaaitaal et al. 2011, Vatsa et al. 2011b). In protoplasts, 1 mM $LaCl_3$ or 5 μM staurosporine completely inhibited the flg22-triggered Ca^{2+} transient, whereas at lower concentrations (50 and 100 μM $LaCl_3$; 100 and 500 nM staurosporine) the response was only partially compromised, as revealed by a delayed Ca^{2+} spike and/or a reduced peak height (**Fig. 3a** and **b**). We extended these measurements and determined half-maximal inhibitory concentrations (IC_{50} values) for protoplasts and seedlings. For both compounds typical sigmoidal dose-response curves were obtained (**Fig. 3c–f**), from which IC_{50} values of 80 μM for $LaCl_3$ and 251 nM for staurosporine were derived for the protoplast system. For seedlings, the corresponding IC_{50} values were 76 μM for $LaCl_3$ (similar to protoplasts) and 1080 nM for staurosporine (ca. four-fold higher than in protoplasts). In sum, these experiments

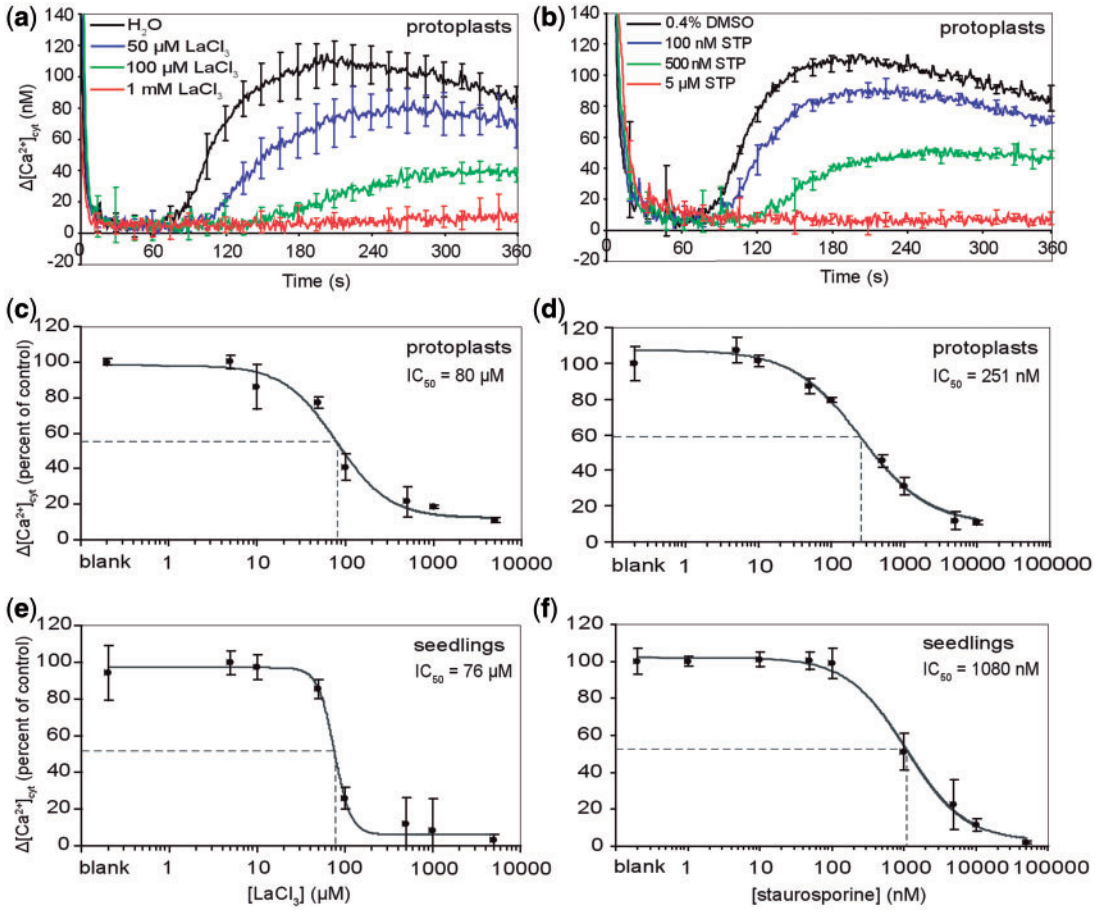

Fig. 3 Comparative pharmacological inhibition of the flg22-triggered Ca^{2+} signatures in *Arabidopsis* seedlings and mesophyll leaf protoplasts. (a, b) $LaCl_3$ and staurosporine inhibit the flg22-induced Ca^{2+} signature in a dose-dependent manner. *Arabidopsis* leaf mesophyll protoplasts isolated from the apoaequorin-expressing Col-0 [pMAQ2] line were pretreated for 10 min with various $LaCl_3$ (0, 50, 100 and 1000 µM) (a) or staurosporine (STP; 0, 100, 500 and 5000 nM) (b) concentrations. The MAMP (1 µM flg22) was injected at the start of the measurements. Data represent $\Delta[Ca^{2+}]_{cyt}$ after normalization to steady state Ca^{2+} levels after MAMP addition and decay of the injection spike, i.e. prior to the genuine elicitor-triggered Ca^{2+} response. Curves are from representative experiments each showing the mean (± SD) of three technical replicates. The experiment was repeated once yielding similar results. (c-f) Dose response curves of flg22-triggered Ca^{2+} signatures and half-maximal inhibitory concentrations (IC_{50} values) of $LaCl_3$ and staurosporine in Col-0 [pMAQ2] seedlings and protoplasts. On the abscissa, logarithmic concentrations of either $LaCl_3$ (c, e) or staurosporine (d, f) were plotted against flg22-triggered $\Delta[Ca^{2+}]_{cyt}$ as percent of control values on the ordinate. Data was obtained at eight different $LaCl_3$ and staurosporine concentrations applied to either Col-0 [pMAQ2]-derived protoplasts (c, d) or Col-0 [pMAQ2] seedlings (e, f). For each treatment, half-maximal inhibitory concentrations (IC_{50}) were calculated as described in Experimental procedures and are indicated by dotted lines. Data shown represent each the mean (±SD) of three technical replicates. The experiment was repeated twice yielding similar results.

demonstrate the suitability of the leaf mesophyll protoplast system for chemical inhibitor studies in the context of MAMP/DAMP-induced Ca^{2+} transients. Generally, similar inhibitor kinetics might be expected in protoplast-based experiments compared to intact seedlings, with the tendency of protoplasts being more sensitive to lower inhibitor concentrations.

Transient expression of the Ca^{2+} reporter apoaequorin in *Arabidopsis* wild-type protoplasts

Next we explored whether transient expression of the Ca^{2+} sensor is a suitable strategy to monitor Ca^{2+} signatures. Therefore, leaf mesophyll protoplasts derived from Col-0 wild type plants were transfected with a plasmid encoding an N-terminally fluorophore (mCherry)-labeled version of the cytoplasmic Ca^{2+} reporter, apoaequorin (mCherry-AEQ). At 12–16 hours post transfection, we detected the specific red fluorescent signal indicating mCherry-AEQ accumulation in the cytoplasm and possibly the nucleus of transfected protoplasts (**Fig. 4a**). When such transfected protoplasts (Col-0 $_{[mCherry\text{-}AEQ]}$) were treated with flg22, the recorded Ca^{2+} transients were comparable to Ca^{2+} signatures obtained with protoplasts from the transgenic *Arabidopsis* line Col-0 [pMAQ2], although we monitored a slightly lower amplitude (90–100 nM *versus* 120–130 nM; **Fig. 4c**). Without MAMP elicitation, protoplasts showed no increase in $[Ca^{2+}]_{cyt}$ over time, demonstrating that the Ca^{2+} signal in the transfected protoplasts is stimulus-dependent (**Fig. 4c**). These results

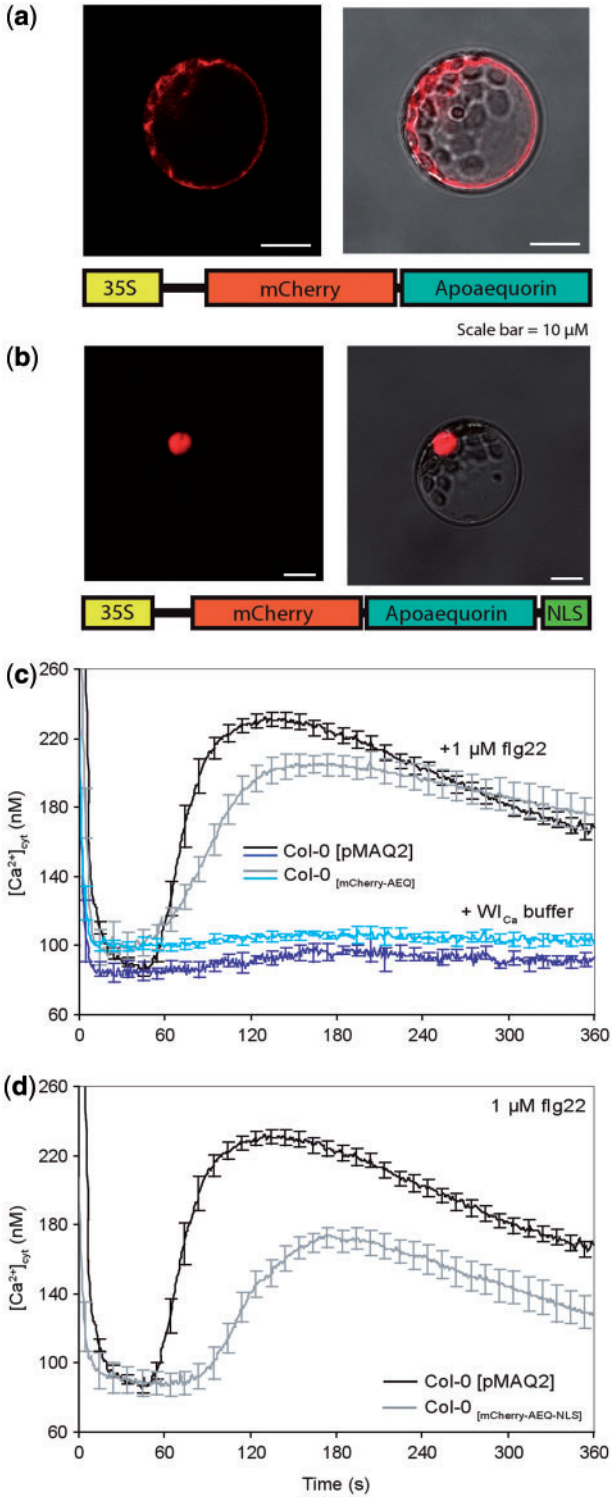

Fig. 4 Transient expression of fluorophore-tagged apoaequorin variants in wild-type *Arabidopsis* leaf mesophyll protoplasts. (a) Transient expression of N-terminally mCherry-tagged apoaequorin (mCherry-AEQ). Left: fluorescence signal; right: fluorescence signal and bright field overlay; bottom: schematic representation of the expression construct (35S, cauliflower mosaic virus 35S promoter). Bar, 10 µm. (b) Transient expression of N-terminally mCherry-tagged apoaequorin harboring a C-terminal nuclear localization signal (mCherry-AEQ-NLS). Left: fluorescence signal; right: fluorescence signal and bright field overlay; bottom: schematic representation of the expression construct (35S, cauliflower mosaic virus 35S promoter; NLS, nuclear localization signal). Bar: 10 µm. (c, d) *Arabidopsis* leaf mesophyll protoplasts were either isolated from the transgenic apoaequorin-expressing Col-0 [pMAQ2] line or Col-0 wild type plants. Col-0-derived protoplasts were either transfected with mCherry-AEQ (c) or mCherry-AEQ-NLS (d). Non-transfected Col-0 [pMAQ2]-derived protoplasts and transfected Col-0-derived protoplasts were either treated with 1 µM flg22 or WI$_{Ca}$ buffer at the start of the measurements. Curves are from representative experiments each showing the mean (± SEM) of three biological replicates and each based on at least three technical replicates, respectively. Note that the black curves (Col-0 [pMAQ2]) in (c) and (d) represent the same data and are identical.

show that the MAMP-induced Ca^{2+} response of mCherry-AEQ-transfected mesophyll protoplasts qualitatively and quantitatively resembles the response of protoplasts isolated from the transgenic Col–0 [pMAQ2] line. The data further indicate that the translational fusion of apoaequorin with the mCherry fluorophore does not affect the activity of the Ca^{2+} sensor.

We also tested a modified version of the mCherry-AEQ reporter construct, which harbors an additional C-terminal nuclear localization signal (NLS) thereby directing the polypeptide to the nucleus (mCherry-AEQ-NLS). The respective fusion protein accumulated in the nuclei of transfected protoplasts with no or only little cytoplasmic localization (**Fig. 4b**). Again, flg22-triggered Ca^{2+} signatures recorded with transfected protoplasts expressing this apoaequorin variant with nuclear localization signal were similar in shape as the response curve obtained with the cytoplasmic apoaequorin version, although the amplitude was somewhat lower under identical experimental conditions ($\Delta[Ca^{2+}]_{cyt}$ ca. 70 nM) than the transients recorded with the cytoplasmic apoaequorin version ($\Delta[Ca^{2+}]_{cyt}$ ca. 120 nM; compare **Fig. 4c** and **d**). Also, the onset of Ca^{2+} influx in the nucleus was delayed by ca. 30 seconds in comparison to the cytoplasmic recordings. This finding is consistent with similar comparative measurements of flg22-induced Ca^{2+} transients in the cytoplasm and nucleus of cultured tobacco cells, although the delay of the nuclear signal in the tobacco system was longer, amounting to a difference in timing of the Ca^{2+} transients of up to 15 min (Lecourieux et al. 2005). Based on results with pharmacological inhibitors the authors of the latter study argued that the rise in nuclear $[Ca^{2+}]$ is unlikely to result from merely the passive diffusion of Ca^{2+} from the cytosol, but may rather originate from an influx from internal stores such as the intermembrane space of the nuclear envelope or the ER-nucleus membrane continuum (Lecourieux et al. 2005).

Transient apoaequorin expression in *bak1-4* mutant protoplasts

Results from a previous report revealed that the increase of $[Ca^{2+}]_{cyt}$ in response to the peptide MAMPs flg22 and elf18, but not in response to the fungal carbohydrate MAMP, chitin, was delayed and reduced in *bak1-3* and *bak1-4* mutants (Ranf et al. 2011). BAK1 acts as a co-receptor of the flg22 receptor, FLS2, and the elf18 receptor, EF-Tu, but not of the chitin

receptor, CERK1 (Gimenez-Ibanez et al. 2009). To unravel whether the differential response seen in seedlings of the *bak1* mutant background can be reproduced in the mesophyll protoplast system, we compared MAMP-induced Ca^{2+}signatures in (1) protoplasts derived from a transgenic aequorin-expressing wild-type line (Col-0 [pMAQ2]), (2) protoplasts isolated from a transgenic aequorin-expressing *bak1-4* mutant line (*bak1-4* [pMAQ2]; Ranf et al. 2011) and (3) protoplasts derived from the *bak1-4* mutant transfected with the apoaequorin-encoding plasmid pMAQ2 (*bak1-4* $_{[pMAQ2]}$). In line with the previous findings (Ranf et al. 2011), the transgenic *bak1-4* [pMAQ2] mutant line showed a delayed and somewhat reduced $[Ca^{2+}]_{cyt}$ signature in response to flg22 (**Fig. 5a**) and elf18 (**Fig. 5b**), but not in response to chitin (**Fig. 5c**), when compared to protoplasts derived from apoaequorin-expressing wild type plants. Importantly, the differential behavior in the *bak1* mutant was faithfully phenocopied by mCherry-AEQ-transfected *bak1-4* mesophyll protoplasts (**Fig. 5**). These data indicate that transient apoaequorin expression in leaf mesophyll protoplasts can be successfully combined with genetic pathway analysis using *Arabidopsis* mutants for protoplast isolation and transfection.

fls2 mutant complementation by transient gene expression in leaf mesophyll protoplasts

To further explore the potential of genetic pathway analysis in the context of MAMP-triggered Ca^{2+} signatures, we speculated that loss-of-gene functions could be restored by transient gene expression in protoplasts. For proof of concept we took advantage of an *Arabidopsis fls2* mutant, in which expression of the pattern recognition receptor FLS2 is completely abolished by a T-DNA insertion (Gómez-Gómez and Boller 2000, Zipfel et al. 2004). Consequently, the *fls2* mutant is insensitive to flg22 but retains responsiveness to other MAMPs. Protoplasts derived from a transgenic apoaequorin-expressing *fls2* T-DNA mutant line (*fls2* [pMAQ2]) were transfected with a plasmid encoding an epitope-tagged FLS2 version under the control of its native promoter (pCAMBIA-FLS2p::FLS2-3xmyc-GFP) and treated with either flg22 or elf18. Non-transfected protoplasts of the apoaequorin-expressing *fls2* mutant were unresponsive to flg22 (**Fig. 6a**) but retained responsiveness to elf18 (**Fig. 6b**), whereas the *FLS2*-transfected protoplasts (*fls2* [pMAQ2] $_{[FLS2p::FLS-3xmyc-GFP]}$) exhibited a flg22-triggered Ca^{2+} signature that was similar to the flg22-induced Ca^{2+} response in protoplasts derived from the apoaequorin-expressing wild-type line (**Fig. 6a**). The slightly different kinetics of the $[Ca^{2+}]_{cyt}$ response obtained in the transfected protoplasts might result from different receptor versions being expressed (wild-type FLS2 *versus* epitope-tagged FLS2) or from different expression levels and thus different receptor quantities in non-transfected and transfected protoplasts. As expected, the Ca^{2+} response to elf18 was indistinguishable in the different types of protoplasts used in this set of experiments (**Fig. 6b**). In conclusion, our data demonstrate that genetic complementation analysis is feasible by combining transient gene expression in mutant protoplasts with luminescence-based measurements of Ca^{2+} signatures.

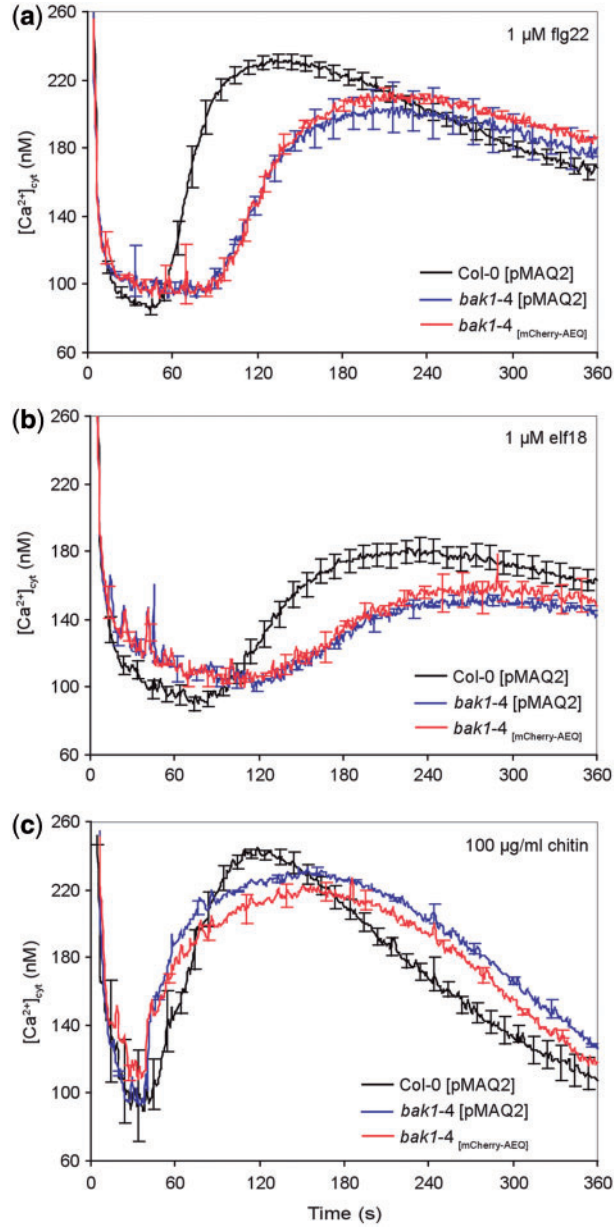

Fig. 5 Transient expression of apoaequorin in *Arabidopsis bak1* leaf mesophyll protoplasts. *Arabidopsis* leaf mesophyll protoplasts isolated from the transgenic apoaequorin-expressing Col-0 [pMAQ2] line (black curves), the transgenic apoaequorin-expressing line with *bak1-4* mutant background (*bak1-4* [pMAQ2]; blue curves) and *bak1-4*-derived protoplasts transfected with mCherry-AEQ (*bak1-4* $_{[mCherry-AEQ]}$; red curves) were treated with 1 µM flg22 (a), 1 µM elf18 (b) or 100 µg/ml chitin (c) at the start of the measurements. Curves are from representative experiments each showing the mean (± SEM) of two biological replicates, all of which are based on at least three technical replicates, respectively.

Discussion

The results presented in this study demonstrate that *Arabidopsis* mesophyll protoplasts represent a versatile and convenient tool to determine MAMP-/DAMP-induced Ca^{2+} signatures in intact plant cells. Apoaequorin-expressing protoplasts largely reflect the $[Ca^{2+}]_{cyt}$ increases in response to

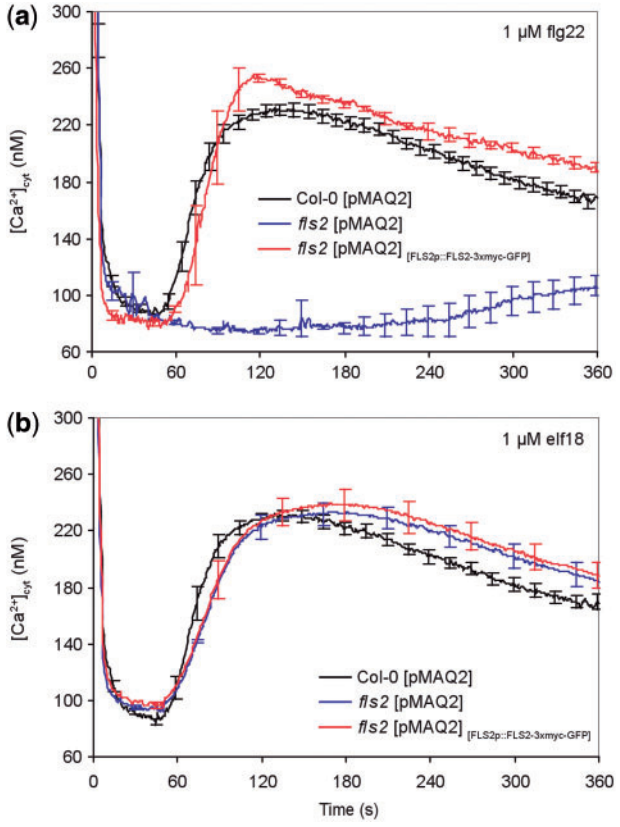

Fig. 6 Genetic complementation by transient gene expression in *Arabidopsis* leaf mesophyll protoplasts. *Arabidopsis* leaf mesophyll protoplasts isolated from the transgenic apoaequorin-expressing Col-0 [pMAQ2] line (black curves), an apoaequorin-expressing line with *fls2* mutant background (*fls2* [pMAQ2]; blue curves), and an apoaequorin-expressing line with *fls2* mutant background transfected with pCAMBIA-FLS2p::FLS2-3xmyc-GFP (*fls2* [pMAQ2]$_{[FLS2p::FLS2\text{-}3xmyc\text{-}GFP]}$; red curves) were treated with either 1 μM flg22 (a) or 1 μM elf18 (b) at the start of the measurements. Curves are from representative experiments each showing the mean (± SEM) of two biological replicates, all of which are based on at least three technical replicates, respectively.

various elicitors seen in whole seedlings, which are typically used to study Ca^{2+} responses in *Arabidopsis*, but also revealed some distinctive features regarding timing, amplitude and recovery phase (**Figs. 1** and **2**; Kwaaitaal et al. 2011, Ranf et al. 2011, Kwaaitaal et al. 2012, Ranf et al. 2012). These differences are unlikely a consequence of the different age of seedlings (2 weeks) and leaves (5 to 6 weeks) used for protoplast preparation since we obtained similar results with protoplasts isolated from mature leaves and protoplasts isolated from seedlings (**Supplementary Fig. 1**). The kinetic differences observed in response to the applied stimuli may thus rather result from the combination of different cell and tissue types in the case of seedlings vs. a single cell type (mesophyll cells) predominating the protoplast preparation. However, roots have previously been shown to provide only a minor contribution to the flg22- and elf18-induced Ca^{2+} signature and a substandard contribution to the chitin- and Pep1-induced Ca^{2+} signature in seedlings (Ranf et al. 2011). Thus, leaf cells including mesophyll cells likely contribute a major proportion to the seedling response. Alternatively or in addition, responses may not be cell-autonomous in seedlings but rather involve feedback control between neighboring cells within the tissue, thereby possibly giving rise to more complex Ca^{2+} patterns.

The faster responsiveness of the seedlings, reaching an earlier maximum of $[Ca^{2+}]_{cyt}$ upon elicitation with flg22 and elf18, was unexpected. Intuitively, one might predict a quicker response in the protoplast system because the applied elicitors (MAMPs/DAMPs) should rapidly diffuse and bind to their exposed cognate plasma membrane-resident receptors of the free-floating, spherical mesophyll protoplasts, which lack at least part of their cell walls. However, epidermal cells of intact seedlings may intrinsically react faster to MAMPs/DAMPs than leaf mesophyll cells. Alternatively, lower levels of PRRs in mesophyll compared to epidermal cells may cause a delayed response. Finally, extracellular Ca^{2+} reservoirs differ in the seedling and protoplast system; while Ca^{2+} may be present at high local concentrations in the apoplastic space of seedlings (possibly varying between 10 μM and 10 mM; Stael et al. 2012), it is provided as homogenous solution in the context of protoplast-based experiments. However, the response of protoplasts was strongly reduced but not completely abolished when Ca^{2+} was omitted from the medium, suggesting that MAMP/DAMP-triggered Ca^{2+} influx remains operative at a wide range of concentrations. The most extreme difference between protoplasts and seedlings in response to treatment with different elicitors was observed with LPS. In contrast to protoplasts, seedlings showed no Ca^{2+} transient upon LPS treatment (**Fig. 2**). Although we used the same batch of LPS throughout our experiments, it remains open whether the lack of a Ca^{2+} response in seedlings truly reflects inherent differences of both systems or whether it relates to different properties of commercial LPS batches/preparations that have previously been reported (S. Ranf, personal communication, Schneider et al. 1997).

An obvious advantage of the protoplast system in comparison to intact seedlings is the reduced complexity of cell types. While many different cell types may contribute to the Ca^{2+} signature seen in seedlings or detached leaves, another experimental system used to conduct aequorin measurements (Grant et al. 2000, Aslam et al. 2009, Qi et al. 2010), leaf mesophyll protoplasts represent a homogenous and adjustable (with regard to the number of cells) type of experimental material. This feature is expected to minimize experimental variation and to confer reproducible data. Isolation of protoplasts usually yields an ample amount of experimental material. Consequently, the homogenous nature of the cell suspension allows direct comparison of different cellular responses upon treatment with different stimuli (e.g. elicitors, hormones, chemicals) using appropriate aliquots. Alternatively, different analytical procedures may be applied to a single batch of protoplasts following treatment with a specific stimulus. The results of such analyses based on homogenous cell/protoplast populations are expected to provide better comparability and reproducibility in comparison to experiments carried out with whole organisms (seedlings). Previous work has shown that also whole seedlings, or shoots and roots separated therefrom, can be used

for protoplast preparation (Zhai et al. 2009, Bargmann and Birnbaum 2010). In combination with subsequent fluorescence-activated cell sorting (FACS) of plant protoplasts, a direct link between the tissue origin and shape of the Ca^{2+} signatures and consecutive downstream responses could be achieved. Cell-type-specific expression of the Ca^{2+} reporter apoaequorin is already available by GAL4 transactivation of the aequorin gene in enhancer trap lines of *Arabidopsis* (Martí et al. 2013). Comparative analysis of the $[Ca^{2+}]_{cyt}$ elevation of these lines at seedling stage and as protoplasts could assist in deciphering the composition and origin of the so far observed $[Ca^{2+}]_{cyt}$ elevations obtained from the transgenic Col-0 [pMAQ2] line, which constitutively expresses apoaequorin without tissue-specificity. These new technical possibilities have the potential to make a marked contribution to the dissection of plant Ca^{2+} signaling pathways, including Ca^{2+} responses triggered by MAMPs/DAMPs.

A particular concern of using protoplasts for MAMP-induced Ca^{2+} measurements might be the liberation of plant cell wall fragments during protoplast preparation and/or the release of cellular content and debris upon undesired lysis of protoplasts during experiments. Both cell wall fragments and cellular debris could potentially act as DAMPs and thereby have an impact on the MAMP-triggered Ca^{2+} responses by either stimulating (priming) or desensitizing the protoplasts for the subsequent MAMP stimulus. The latter could be an alternative explanation for the delayed flg22- or elf-18-induced response of protoplasts (**Figs. 1** and **2a**, **b**). However, treatment with the endogenous elicitors Pep1 or the fungal MAMP chitin did not result in delayed Ca^{2+} responses of protoplasts in comparison to seedlings grown in hydroponic culture (**Fig. 2b** and **c**).

The protoplasts were prepared by a non-sterile isolation procedure; thus microbial contamination was unavoidable. Indeed, longer storage (e.g. overnight) of protoplasts at room temperature often resulted in a marked decline of the recorded Ca^{2+} flux, which we associated with enhanced bacterial growth in the protoplast-containing medium (**Supplementary Fig. 2**). By contrast, upon overnight storage at 4°C protoplasts retained their responsiveness to MAMP treatment and produced reliable and reproducible Ca^{2+} traces (**Supplementary Fig. 2**). Thus, protoplasts apparently remain viable and retain their capacity for generating Ca^{2+} transients for an extended time period, provided that bacterial contamination and growth is minimized, which enables their application in large-scale and time-consuming experiments.

Protoplasts can also be used for pharmacological inhibitor studies (**Fig. 3**) and genetic pathway analysis (**Figs. 4–6**). In fact, the protoplast system may be advantageous for inhibitor studies since some chemicals might be taken up more easily than by intact seedlings owing to the greater accessible surface area and the at least partially lacking cell walls. We conducted a comparative analysis in protoplasts and seedlings with two well-characterized inhibitors of Ca^{2+} mediated responses, the Ca^{2+} channel blocker $LaCl_3$ and the kinase inhibitor staurosporine (**Fig. 3**). We determined a similar IC_{50} value for $LaCl_3$ in both systems, which is not unexpected, since this Ca^{2+} blocker acts on the extracellular face of plasma membrane-localized Ca^{2+} channels. La^{3+} ions bind to the pore of Ca^{2+} channels, resulting in pore occlusion (Doering and Zamponi 2003). This process is dependent on the physical interaction between the La^{3+} ion and the channel pore, which should be independent of the biological system under examination. By contrast, staurosporine as pan-specific protein kinase inhibitor (Karaman et al. 2008) blocks a wide range of ATP-dependent mechanisms. Therefore it may interfere with diverse ATP-dependent and/or kinase-mediated processes, including to defense-associated signaling processes MAMP-induced cytoplasmic receptor kinase activities. In contrast to $LaCl_3$, staurosporine has to enter cells to exert its effect. This process may take longer or may be less effective in cells of the tissue interior. In addition, unspecific binding to other targets or cellular components such as the cell wall may reduce the effective intracellular concentration. In any case, the apparent IC_{50} value for staurosporine was about four times higher in seedlings than in protoplasts (1080 nM vs. 251 nM, respectively).

For the analysis of genetic pathways, the presented system offers the possibility to transiently express the apoaequorin Ca^{2+} reporter in different genetic backgrounds (**Figs. 4–6**). This option renders mutant analysis faster and much more effective, since it alleviates researchers from the otherwise necessary introgression of transgenic apoaequorin reporter constructs into suitable plant lines by either transformation or crossing. Available single or higher order mutants can directly be used for protoplast isolation in combination with transfection, saving considerable time in comparison to conventional modes of analysis. For example, recent studies uncovered cyclic nucleotide-gated channels (Clough et al. 2000, Ali et al. 2007, Ma et al. 2009) and ionotropic glutamate receptor (iGluR)-like channels (Kwaaitaal et al. 2011, Vatsa et al. 2011a, Kwaaitaal et al. 2012, Manzoor et al. 2013, Li et al. 2013) as candidates that could mediate Ca^{2+} influx during plant-microbe interactions. Given that these proteins are encoded by medium-sized gene families, comprising 20 members each in *Arabidopsis*, conventional genetic analysis *via* introgression of the reporter construct into each of the different mutants is tedious and time-consuming. Besides for the identification of the actual channels, the procedure can also be used to study the role of presumed Ca^{2+} signal transduction components. It offers further the possibility to verify the presumed effect of mutants by complementation analysis (**Fig. 6**), saving the need for additional independent mutant alleles to prove the contribution of a particular gene in Ca^{2+} signaling. Co-transfection of multiple plasmids enables co-expression of apoaequorin reporter constructs together with gene complementation constructs within the same cell, further extending the options of mutant analysis. Thus, candidate genes can be tested and identified more quickly using the protoplast system and eventually verified by stable transgenic lines in a more targeted approach.

An additional aspect of the protoplast system is the possibility to deploy flexibly Ca^{2+} sensor variants with improved sensitivity (Dikici et al. 2009), defined subcellular localization (**Fig. 4**), or other specific features. The usage of reporter variants with particular subcellular localization might be useful to resolve the spatial distribution of Ca^{2+} patterns. Mehlmer and co-workers

recently described a modular set of apoaequorin plant expression vectors that can be used to target the Ca^{2+} sensor to different subcellular compartments such as the nucleus, nucleolus, mitochondria, chloroplasts and the plasma membrane (Mehlmer et al. 2012). With such a set of expression vectors at hand, protoplast-based experiments can rapidly unravel the origin and subcellular spreading of Ca^{2+} signatures in any genetic background.

Materials and methods

Plant material

In this study we used *Arabidopsis thaliana* accession Col-0, Col-0 expressing cytosolic apoaequorin (line Col-0 [pMAQ2]; Knight et al. 1991), the mutants *bak1*–4 (At4g33430, line SALK_116202; Chinchilla et al. 2007), and *bak1*–4 expressing cytosolic apoaequorin (line *bak1-4* [pMAQ2]; Ranf et al. 2011), the mutant *fls2* (At5g46330; line SAIL_691C4; Zipfel et al. 2004) and *fls2* expressing cytosolic apoaequorin (line *fls2* [pMAQ2]; Frei dit Frey et al. 2012). For protoplast isolation plants were grown in soil substrate for 4 to 6 weeks at a day/night cycle of 10/14 h in a growth chamber at 23°C/22°C day/night temperature and a relative humidity of 60%. For whole seedling assays, *Arabidopsis* Col-0 [pMAQ2] seeds were surface-sterilized and transferred (one seed per well) to white 96-well microplates (PerkinElmer, Waltham, MA, USA) containing 160 µl of MS basal salt medium (Murashige and Skoog 1962) supplemented with 0.25% sucrose and vitamins (Duchefa Biochemie, Haarlem, The Netherlands). The seedlings were grown for 14 days in a growth chamber with 16 h light (at 21°C), 8 h dark (at 19°C) before further analysis.

Cloning of mCherry-apoaequorin and mCherry-apoaequorin-NLS fusion constructs

The apoaequorin (*AEQ*) coding sequence was PCR-amplified from genomic DNA isolated from seedlings of the Col-0 [pMAQ2] line using primers AEQ01_F (5′-ATGACCAGCGAACAATACTCAGT-3′) and AEQ01_R (5′-TTAGG GGACAGCTCCACCGTA-3′). To generate the corresponding Gateway® (www.lifetechnologies.com) entry clone, the PCR product was used as a template in a second PCR using primers AEQ_GW_F (5′-GGGGACAAGTTTGTACAAAAAAG CAGGCTCCATGACCAGCGAACAATACTCAGT-3′) and AEQ_GW_R (5′-GGG GACCACTTTGTACAAGAAAGCTGGGTCTTAGGGGACAGCTCCACC-3′). The product was inserted into the pDONR201 entry vector using the Gateway BP reaction. To generate the AEQ-NLS entry clone, the SV40 nuclear localization signal was attached to the *AEQ* coding sequence using the primers AEQ_RNLS 5′-CTATCCTCCAACCTTTCTCTTCTTCTTAGGGGGGACAGCTCCACCGTA-3′ and AEQ01_F (see above). In a subsequent PCR the Gateway recombination sequences were added to the AEQ-NLS sequence using primers: AEQ_GW_F and AEQNLS_GW_R 5′-GGGGACCACTTTGTACAAGAAAGCTGGGTCCTATC CTCCAACCTTTCTCTTCTTC-3′, and this product was also inserted into the pDONR201 entry vector by the BP reaction. Using the Gateway LR reaction, the *AEQ* and *AEQ-NLS* coding sequences were subsequently inserted into the destination vector p35S-mCherry-Gateway.

Protoplast isolation and transfection

Protoplasts were isolated and transfected as previously described (Yoo et al. 2007). All plasmids used for transfection (p35S::mCherry–AEQ, p35S::mCherry–AEQ–NLS or FLS2p::FLS2–3xmyc–GFP) were propagated in *Escherichia coli* DH5α strains and purified with the NucleoBond® Xtra Midi kit (Macherey-Nagel, Düren, Germany). Transfection efficiency was calculated by counting several times the total number of protoplasts in the field of view of a microscope, and then counting the number of protoplasts showing red fluorescence due to successful transfection and resulting expression of mCherry-apoaequorin. The protoplast transfection efficiency was on average 65.8% ± 10.8% (mean ± SD).

Quantitative Ca^{2+} measurements

After transfection, protoplasts were stored in 2 ml batches containing approximately 4×10^5 protoplasts overnight at 4°C in washing and incubation solution (WI solution; 4 mM MES pH 5.7, 0.5 M mannitol, 20 mM KCl; Yoo et al. 2007) supplemented with 2 mM $CaCl_2$ (WI_{Ca}). On the following day, coelenterazine (Biosynth, Staad, Switzerland) was added to 10 µM final concentration (from a 5 mM stock solution in methanol) and protoplasts were incubated for one to four hours. Then, 100 µl of protoplast solution in WI_{Ca} buffer containing approximately 2×10^4 protoplasts were loaded into single wells of black 96-well microplates (Perkin Elmer, Waltham, MA, USA) and incubated 30 min in the dark before starting the Ca^{2+} measurements.

For seedlings, after 14 days the growth medium was removed and replaced by 100 µl ddH_2O containing 10 µM coelenterazine and incubated overnight in the dark. The next day, the liquid was replaced by 100 µl of ddH_2O and the seedlings were incubated 30 min in the dark before starting the Ca^{2+} measurements.

The Ca^{2+}-dependent bioluminescence was quantified in a Centro X^3 LB960 or a TriStar^2 LB 942 microplate reader (Berthold Technologies, Bad Wildbad, Germany). To determine the high resolution kinetics of the Ca^{2+} influx in protoplast suspensions and individual seedlings in single wells, the response was initiated by automatic injection of 5-fold concentrated MAMP solution (in WI_{Ca} for protoplasts or ddH_2O for seedlings) to give a final concentration of 1 µM flg22, 1 µM elf18, 1 µM Pep1, 100 µg/ml chitin or 10 µg/ml LPS. These concentrations correspond to those used in previous studies (Zeidler et al. 2004, Kwaaitaal et al. 2011, Ranf et al. 2011). Luminescence was continuously recorded in single wells and integrated over 1 s intervals for a total time period of at least 360 s. For IC_{50} determination in seedlings, instead of monitoring individual seedlings, half a microplate (48 samples) was monitored in parallel. Luminescence from each single well was integrated for 0.25 s and the cycle over all wells was repeated every 30 s. After 30 min of pre-incubation (e.g. treatment with inhibitors as described below), the response was initiated by automatic injection of 5-fold concentrated MAMP to provide a final concentration of 1 µM flg22 as described above, and the luminescence was recorded for additional 30 min. The second half of a microplate was used in the same manner subsequently. For each treatment, at least three technical replicates were determined (recorded subsequently) and the resulting three $[Ca^{2+}]$ traces averaged to provide the result of one experiment. Each experiment was repeated at least 2 or 3 times yielding similar results. Given the fact that the absolute value (i.e. peak height) of the Ca^{2+} response (not so much the peak position along the time axis) was dependent on seedling size and its physiological (growth) conditions and because individual $[Ca^{2+}]$ traces relied on recordings of single seedlings, all comparative experiments were carried out with plant material from the same growth batch.

To calculate absolute cytoplasmic Ca^{2+} concentrations ($[Ca^{2+}]_{cyt}$), the remaining aequorin in each sample (microplate well) was discharged by adding 100 µl of 2 M $CaCl_2$ in 20% ethanol using an injector of the microplate reader. The luminescence was continuously monitored for at least 30 s in single well kinetics or repeatedly every 30 s for a period of 30 min in multiple parallel assays using half a microplate. Final $[Ca^{2+}]_{cyt}$ were calculated as previously described (Rentel and Knight 2004).

Protoplast samples typically showed very strong luminescent signals. To avoid signal saturation, especially during normalization, protoplasts were measured in plates with black well walls, which reduces overall signal strength and improves the signal-to-noise ratio. In general, similar results were achieved when using plates with white well walls.

The elicitors used in these assays, flg22, elf18 and Pep1, were prepared as 10 mM or 1 mM stock solutions in water and stored at −80°C. Working solutions were freshly diluted before use. The chitin solution was prepared and stored as described before (Kwaaitaal et al. 2011). A stock solution of 1 mg/ml of lipopolysaccharides (LPS) from *Escherichia coli* (L3012, Sigma, Munich, Germany) was stored at 4°C.

Pharmacological tests and IC_{50} determination

For IC_{50} determination, aliquots of coelenterazine-loaded protoplasts isolated from the Col-0 [pMAQ2] line or individual coelenterazine-loaded Col-0 [pMAQ2] seedlings in single wells were pre-incubated for 10 min with either staurosporine or $LaCl_3$ (Sigma, Munich, Germany) at different final concentrations, limiting the added DMSO (as solvent for staurosporine) to <0.4% in protoplasts and <1% in seedlings. Protoplasts were pretreated with inhibitors for 10 min and seedlings for 30 min prior MAMP application. The maximum of the MAMP-triggered $[Ca^{2+}]_{cyt}$ response of each treatment was calculated as the

percentage of corresponding control values without inhibitor. Ca^{2+} transients were compared between treatments within one experiment. The IC_{50} values were calculated following the guidelines for accurate EC_{50}/IC_{50} estimation (Sebaugh 2011) using nonlinear regression to fit a 4-parameter logistic model (1) to the data, which describes a sigmoid response pattern.

$$Y = d + \frac{a-d}{1+\left(\frac{X}{c}\right)^{b}} \quad (1)$$

Y describes the activity as percentage of the control and *X* the concentration of the inhibitor. The lower and upper plateau of the curve are defined by *a* and *d*, respectively, whereas parameter *c* is the concentration at which *Y* is halfway between *a* and *d*. The slope factor *b* describes the steepness of the linear portion of the curve. For solving the equation we defined the MAMP-triggered control (+/- SD) as *d* and the non-induced control (+/- SD) as *a*. The equation was solved by applying Solver (MS Excel) to the formula (1) obtaining estimates of *a*, *b*, *c* and *d* with the least root mean square error for the measured and corresponding calculated activities.

Supplementary data

Supplementary data are available at PCP online.

Funding

This work was supported by the Max Planck Society and the Excellence Initiative of the German federal and state governments (seed fund provided to R.P. by the RWTH Aachen University). J.M. was recipient of an IMPRS doctoral fellowship (Max Planck Institute for Plant Breeding Research, Cologne).

Acknowledgments

We are grateful to Marc Knight and Dierk Scheel for making available the Col-0 [pMAQ2] apoaequorin reporter line and to Nicolas Frei dit Frey and Silke Robatzek for providing the *fls2* mutant (with and without the pMAQ2 transgene) and the *FLS2* complementation construct (pCAMBIA-FLS2p::FLS2-3xmyc-GFP). Dierk Scheel and Stefanie Ranf are acknowledged for sharing the apoaequorin-expressing *bak1-4* mutant, and we thank Yusuke Saijo for the supply of Pep1 elicitor.

Disclosures

The authors have no conflicts of interest to declare.

References

Ali, R., Ma, W., Lemtiri-Chlieh, F., Tsaltas, D., Leng, Q., Bodman, S. et al. (2007) Death don't have no mercy and neither does calcium: Arabidopsis CYCLIC NUCLEOTIDE GATED CHANNEL2 and innate immunity. *Plant Cell* 19: 1081–1095.

Asai, T., Tena, G., Plotnikova, J., Willmann, M.R., Chiu, W.L., Gomez-Gomez, L. et al. (2002) MAP kinase signalling cascade in *Arabidopsis* innate immunity. *Nature* 415: 977–983.

Aslam, S.N., Erbs, G., Morrissey, K.L., Newman, M.A., Chinchilla, D., Boller, T. et al. (2009) Microbe-associated molecular pattern (MAMP) signatures, synergy, size and charge. influences on perception or mobility and host defence responses. *Mol. Plant Pathol.* 10: 375–387.

Bargmann, B.O. and Birnbaum, K.D. (2010) Fluorescence activated cell sorting of plant protoplasts. *J. Vis. Exp.* 36: 1673.

Blume, B., Nürnberger, T., Nass, N. and Scheel, D. (2000) Receptor-mediated increase in cytoplasmic free calcium required for activation of pathogen defense in parsley. *Plant Cell* 12: 1425–1440.

Boudsocq, M., Willmann, M.R., McCormack, M., Lee, H., Shan, L.B., He, P. et al. (2010) Differential innate immune signalling via Ca^{2+} sensor protein kinases. *Nature* 464: 418–422.

Bush, D.S. (1995) Calcium regulation in plant cells and its role in signaling. *Annu. Rev. Plant Physiol. Plant Mol. Biol.* 46: 95–122.

Carpaneto, A., Ivashikina, N., Levchenko, V., Krol, E., Jeworutzki, E., Zhu, J.-K. et al. (2007) Cold transiently activates calcium-permeable channels in Arabidopsis mesophyll cells. *Plant Physiol.* 143: 487–494.

Chinchilla, D., Zipfel, C., Robatzek, S., Kemmerling, B., Nürnberger, T., Jones, J.D.G. et al. (2007) A flagellin-induced complex of the receptor FLS2 and BAK1 initiates plant defence. *Nature* 448: 497–500.

Clough, S.J., Fengler, K.A., Yu, I.C., Lippok, B., Smith, R.K. and Bent, A.F. (2000) The Arabidopsis *dnd1 'defense, no death'* gene encodes a mutated cyclic nucleotide-gated ion channel. *Proc. Natl Acad. Sci. USA* 97: 9323–9328.

Davey, M.R., Anthony, P., Power, J.B. and Lowe, K.C. (2005) Plant protoplasts: status and biotechnological perspectives. *Biotechnol. Adv.* 23: 131–171.

Demidchik, V., Essah, P.A. and Tester, M. (2004) Glutamate activates cation currents in the plasma membrane of *Arabidopsis* root cells. *Planta* 219: 167–175.

Dikici, E., Qu, X., Rowe, L., Millner, L., Logue, C., Deo, S.K. et al. (2009) Aequorin variants with improved bioluminescence properties. *Proc. SPIE* 22: 243–248.

Doering, C.J. and Zamponi, G.W. (2003) Molecular pharmacology of high voltage-activated calcium channels. *J. Bioenerg. Biomembr.* 35: 491–505.

Felix, G., Duran, J.D., Volko, S. and Boller, T. (1999) Plants have a sensitive perception system for the most conserved domain of bacterial flagellin. *Plant J.* 18: 265–276.

Frei dit Frey, N., Mbengue, M., Kwaaitaal, M., Nitsch, L., Altenbach, D. et al. (2012) Plasma membrane calcium ATPases are important components of receptor-mediated signaling in plant immune responses and development. *Plant Physiol.* 159: 798–809.

Gelvin, S.B. (2003) *Agrobacterium*-mediated plant transformation: the biology behind the 'gene-jockeying' tool. *Microbiol. Mol. Biol. Rev.* 67: 16–37.

Gilroy, S., Hughes, W.A. and Trewavas, A.J. (1986) The measurement of intracellular calcium levels in protoplasts from higher plant cells. *FEBS Lett.* 199: 217–221.

Gilroy, S., Hughes, W.A. and Trewavas, A.J. (1989) A comparison between quin-2 and aequorin as indicators of cytoplasmic calcium levels in higher plant cell protoplasts. *Plant Physiol.* 90: 482–491.

Gimenez-Ibanez, S., Hann, D.R., Ntoukakis, V., Petutschnig, E., Lipka, V. and Rathjen, J.P. (2009) AvrPtoB targets the LysM receptor kinase CERK1 to promote bacterial virulence on plants. *Curr. Biol.* 19: 423–429.

Gómez-Gómez, L. and Boller, T. (2000) FLS2: An LRR receptor-like kinase involved in the perception of the bacterial elicitor flagellin in *Arabidopsis*. *Mol. Cell* 5: 1003–1011.

Grant, M., Brown, I., Adams, S., Knight, M., Ainslie, A. and Mansfield, J. (2000) The *RPM1* plant disease resistance gene facilitates a rapid and sustained increase in cytosolic calcium that is necessary for the oxidative burst and hypersensitive cell death. *Plant J.* 23: 441–450.

Gust, A.A., Biswas, R., Lenz, H.D., Rauhut, T., Ranf, S., Kemmerling, B. et al. (2007) Bacteria-derived peptidoglycans constitute pathogen-associated molecular patterns triggering innate immunity in *Arabidopsis*. *J. Biol. Chem.* 282: 32338–32348.

Haley, A., Russell, A.J., Wood, N., Allan, A.C., Knight, M., Campbell, A.K. et al. (1995) Effects of mechanical signaling on plant cell cytosolic calcium. *Proc. Natl Acad. Sci. USA* 92: 4124–4128.

Huffaker, A., Pearce, G. and Ryan, C.A. (2006) An endogenous peptide signal in *Arabidopsis* activates components of the innate immune response. *Proc. Natl Acad. Sci. USA* 103: 10098–10103.

Jeworutzki, E., Roelfsema, M.R.G., Anschütz, U., Krol, E., Elzenga, J.T.M., Felix, G. et al. (2010) Early signaling through the Arabidopsis pattern recognition receptors FLS2 and EFR involves Ca^{2+}-associated opening of plasma membrane anion channels. *Plant J.* 62: 367–378.

Karaman, M.W., Herrgard, S., Treiber, D.K., Gallant, P., Atteridge, C.E. et al. (2008) A quantitative analysis of kinase inhibitor selectivity. *Nat. Biotechnol.* 26: 127–132.

Keinath, N.F., Kierszniowska, S., Lorek, J., Bourdais, G., Kessler, S.A., Shimosato-Asano, H. et al. (2010) PAMP (Pathogen-Associated Molecular Pattern)-induced changes in plasma membrane compartmentalization reveal novel components of plant immunity. *J. Biol. Chem.* 285: 39140–39149.

Kim, B.H., Kim, S.Y. and Nam, K.H. (2013) Assessing the diverse functions of BAK1 and its homologs in Arabidopsis, beyond BR signaling and PTI responses. *Mol. Cells* 35: 7–16.

Knight, H., Trewavas, A.J. and Knight, M.R. (1997) Calcium signalling in *Arabidopsis thaliana* responding to drought and salinity. *Plant J.* 12: 1067–1078.

Knight, M.R., Campbell, A.K., Smith, S.M. and Trewavas, A.J. (1991) Transgenic plant aequorin reports the effects of touch and cold-shock and elicitors on cytoplasmic calcium. *Nature* 352: 524–526.

Kurusu, T., Hamada, H., Sugiyama, Y., Yagala, T., Kadota, Y. et al. (2011) Negative feedback regulation of microbe-associated molecular pattern-induced cytosolic Ca^{2+} transients by protein phosphorylation. *J. Plant Res.* 124: 415–424.

Kwaaitaal, M., Huisman, R., Maintz, J., Reinstädler, A. and Panstruga, R. (2011) Ionotropic glutamate receptor (iGluR)-like channels mediate MAMP-induced calcium influx in *Arabidopsis thaliana*. *Biochem. J.* 440: 355–365.

Kwaaitaal, M., Maintz, J., Cavdar, M. and Panstruga, R. (2012) On the ligand binding profile and desensitization of plant ionotropic glutamate receptor (iGluR)-like channels functioning in MAMP-triggered Ca^{2+} influx. *Plant Signal. Behav.* 7: 1373–1377.

Lecourieux, D., Lamotte, O., Bourque, S., Wendehenne, D., Mazars, C., Ranjeva, R. et al. (2005) Proteinaceous and oligosaccharidic elicitors induce different calcium signatures in the nucleus of tobacco cells. *Cell Calcium* 38: 527–538.

Lecourieux, D., Mazars, C., Pauly, N., Ranjeva, R. and Pugin, A. (2002) Analysis and effects of cytosolic free calcium increases in response to elicitors in *Nicotiana plumbaginifolia* cells. *Plant Cell* 14: 2627–2641.

Lecourieux, D., Raneva, R. and Pugin, A. (2006) Calcium in plant defence-signalling pathways. *New Phytol.* 171: 249–269.

Li, F., Wang, J., Ma, C., Zhao, Y., Wang, Y., Hasi, A. et al. (2013) Glutamate receptor-like channel3.3 is involved in mediating glutathione-triggered cytosolic calcium transients, transcriptional changes, and innate immunity responses in Arabidopsis. *Plant Physiol.* 162: 1497–1509.

Liu, T., Liu, Z., Song, C., Hu, Y., Han, Z. et al. (2012) Chitin-induced dimerization activates a plant immune receptor. *Science* 336: 1160–1164.

Ma, W., Qi, Z., Smigel, A., Walker, R.K., Verma, R. and Berkowitz, G.A. (2009) Ca^{2+}, cAMP, and transduction of non-self perception during plant immune responses. *Proc. Natl. Acad. Sci. USA* 106: 20995–21000.

Manzoor, H., Kelloniemi, J., Chiltz, A., Wendehenne, D., Pugin, A., Poinssot, B. et al. (2013) Involvement of the glutamate receptor AtGLR3.3 in plant defense signaling and resistance to *Hyaloperonospora arabidopsidis*. *Plant J.* 76: 466–480.

Martí, M.C., Stancombe, M.A. and Webb Alex, A.R. (2013) Cell- and stimulus type-specific intracellular free Ca^{2+} signals in Arabidopsis. *Plant Physiol.* 163: 625–634.

Mazars, C., Thion, L., Thuleau, P., Graziana, A., Knight, M.R., Moreau, M. et al. (1997) Organization of cytoskeleton controls the changes in cytosolic calcium of cold-shocked *Nicotiana plumbaginifolia* protoplasts. *Cell Calcium* 22: 413–420.

McAinsh, M.R. and Pittman, J.K. (2009) Shaping the calcium signature. *New Phytol.* 181: 275–294.

McCourt, P. and Desveaux, D. (2010) Plant chemical genetics. *New Phytol.* 185: 15–26.

Mehlmer, N., Parvin, N., Hurst, C.H., Knight, M.R., Teige, M. and Vothknecht, U.C. (2012) A toolset of aequorin expression vectors for *in planta* studies of subcellular calcium concentrations in *Arabidopsis thaliana*. *J. Exp. Bot.* 63: 1751–1761.

Miya, A., Albert, P., Shinya, T., Desaki, Y., Ichimura, K., Shirasu, K. et al. (2007) CERK1, a LysM receptor kinase, is essential for chitin elicitor signaling in *Arabidopsis*. *Proc. Natl Acad. Sci. USA* 104: 19613–19618.

Murashige, T. and Skoog, F. (1962) A revised medium for rapid growth and bio assays with tobacco tissue cultures. *Physiol. Plant.* 15: 473–497.

Newman, M.-A., Sundelin, T., Nielsen, J.T. and Erbs, G. (2013) MAMP (microbe-associated molecular pattern) triggered immunity in plants. *Front. Plant Sci.* 4: 139.

Panstruga, R. (2004) A golden shot. How ballistic single cell transformation boosts the molecular analysis of cereal-mildew interactions. *Mol. Plant Pathol.* 5: 141–148.

Petutschnig, E.K., Jones, A.M.E., Serazetdinova, L., Lipka, U. and Lipka, V. (2010) The lysin motif receptor-like kinase (LysM-RLK) CERK1 is a major chitin-binding protein in *Arabidopsis thaliana* and subject to chitin-induced phosphorylation. *J. Biol. Chem.* 285: 28902–28911.

Qi, Z., Verma, R., Gehring, C., Yamaguchi, Y., Zhao, Y., Ryan, C.A. et al. (2010) Ca^{2+} signaling by plant *Arabidopsis thaliana* Pep peptides depends on AtPepR1, a receptor with guanylyl cyclase activity, and cGMP-activated Ca^{2+} channels. *Proc. Natl Acad. Sci. USA* 107: 21193–21198.

Ranf, S., Eschen-Lippold, L., Pecher, P., Lee, J. and Scheel, D. (2011) Interplay between calcium signalling and early signalling elements during defence responses to microbe- or damage-associated molecular patterns. *Plant J.* 68: 100–113.

Ranf, S., Grimmer, J., Poeschl, Y., Pecher, P., Chinchilla, D., Scheel, D. et al. (2012) Defense-related calcium signaling mutants uncovered via a quantitative high-throughput screen in *Arabidopsis thaliana*. *Mol. Plant* 5: 115–130.

Rentel, M.C. and Knight, M.R. (2004) Oxidative stress-induced calcium signaling in Arabidopsis. *Plant Physiol.* 135: 1471–1479.

Schneider, K., Wells, B., Dolan, L. and Roberts, K. (1997) Structural and genetic analysis of epidermal cell differentiation in *Arabidopsis* primary roots. *Development* 124: 1789–1798.

Sebaugh, J.L. (2011) Guidelines for accurate EC50/IC50 estimation. *Pharm. Stat.* 10: 128–134.

Stael, S., Wurzinger, B., Mair, A., Mehlmer, N., Vothknecht, U.C. and Teige, M. (2012) Plant organellar calcium signalling: an emerging field. *J. Exp. Bot.* 63: 1525–1542.

Vadassery, J., Ranf, S., Drzewiecki, C., Mithöfer, A., Mazars, C., Scheel, D. et al. (2009) A cell wall extract from the endophytic fungus *Piriformospora indica* promotes growth of Arabidopsis seedlings and induces intracellular calcium elevation in roots. *Plant J.* 59: 193–206.

Vatsa, P., Chiltz, A., Bourque, S., Wendehenne, D., Garcia-Brugger, A. and Pugin, A. (2011a) Involvement of putative glutamate receptors in plant defence signaling and NO production. *Biochimie* 93: 2095–2101.

Vatsa, P., Chiltz, A., Luini, E., Vandelle, E., Pugin, A. and Roblin, G. (2011b) Cytosolic calcium rises and related events in ergosterol-treated *Nicotiana* cells. *Plant Physiol. Biochem.* 49: 764–773.

Wheeler, G.L. and Brownlee, C. (2008) Ca^{2+} signalling in plants and green algae—changing channels. *Trends Plant Sci.* 13: 506–514.

Yamaguchi, Y., Huffaker, A., Bryan, A.C., Tax, F.E. and Ryan, C.A. (2010) PEPR2 is a second receptor for the Pep1 and Pep2 peptides and contributes to defense responses in *Arabidopsis*. *Plant Cell* 22: 508–522.

Yoo, S.-D., Cho, Y.-H. and Sheen, J. (2007) *Arabidopsis* mesophyll protoplasts: a versatile cell system for transient gene expression analysis. *Nat. Protoc.* 2: 1565–1572.

Zeidler, D., Zähringer, U., Gerber, I., Dubery, I., Hartung, T., Bors, W. et al. (2004) Innate immunity in *Arabidopsis thaliana*: lipopolysaccharides activate nitric oxide synthase (NOS) and induce defense genes. *Proc. Natl Acad. Sci. USA* 101: 15811–15816.

Zhai, Z., Jung, H.-I. and Vatamaniuk, O.K. (2009) Isolation of protoplasts from tissues of 14-day-old seedlings of *Arabidopsis thaliana*. *J. Vis. Exp.* 30: 1149.

Zipfel, C., Robatzek, S., Navarro, L., Oakeley, E.J., Jones, J.D.G., Felix, G. et al. (2004) Bacterial disease resistance in Arabidopsis through flagellin perception. *Nature* 428: 764–767.